

Quantum Phase Transition with a Simple Variational Ansatz

Y. Lutsyshyn,^{1,*} G. E. Astrakharchik,^{2,†} C. Cazorla,³ and J. Boronat^{2,†}

¹*Institut für Physik, Universität Rostock, 18051 Rostock, Germany*

²*Departament de Física i Enginyeria Nuclear, Universitat Politècnica de Catalunya, Campus Nord B4-B5, E-08034 Barcelona, Spain*

³*School of Materials Science and Engineering, University of New South Wales, Sydney, NSW 2052, Australia*

(Dated: October 21, 2021)

We study the zero-temperature quantum phase transition between liquid and hcp solid ^4He . We use the variational method with a simple yet exchange-symmetric and fully explicit wavefunction. It is found that the optimized wavefunction undergoes spontaneous symmetry breaking and describes the quantum solidification of helium at 22 atm. The explicit form of the wavefunction allows to consider various contributions to the phase transition. We find that the employed wavefunction is an excellent candidate for describing both a first-order quantum phase transition and the ground state of a Bose solid.

Properties of solid ^4He have regained attention due to a host of unexpected physics discovered in the past decade [1–5]. Most of the new features occur close to absolute zero and are believed to be primarily driven by quantum effects. Consequently, the solidification of ^4He came under renewed scrutiny. The role of quantum statistics in the transition location has been recently revisited in Ref. [6]. At small but non-zero temperatures, indistinguishability of particles destabilizes the quantum solid. Distinguishable particles, on the other hand, would solidify even at low pressures, with the phase diagram reminiscent of the Pomeranchuk effect [7, 8]. The feature was dubbed in [6] as thermocrystallization. A similar effect was seen numerically for the Wigner-crystallization of a 2D Coulomb system [9]. The solidification of ^4He at zero temperature was revisited in Ref. [10] with the density functional theory (DFT). Results were improved comparing with previous DFT studies.

In this Letter, we show that the quantum solidification of ^4He can be considered variationally, with a single explicit wavefunction which selects the phase through optimization of the thermodynamic potential. Quite surprisingly, we find that the phase transition is predicted properly, given the relative simplicity of the wavefunction. While the variational treatment is used for quantum phase transitions at the mean-field level [11], it is relatively uncommon that a (discontinuous) transition can be described with a microscopic wavefunction.

At zero temperature, the phases of ^4He can be studied in an essentially exact form with a family of projector methods, including Green’s-function Monte Carlo [12, 13], diffusion Monte Carlo [14], and path integral ground state Monte Carlo [15]. These methods properly describe the phase transition in helium, and can provide insight on the nature of its ground state [16, 17].

Variational calculations with shadow-type wavefunctions (SWF) [18] provide accurate results both for the liquid and solid phases of ^4He [18, 19], and describe the transition [20–22] and coexistence [23] between the two phases. The SWF can be seen as representing a single step of a projection calculation [18]. The projection is carried out by performing the numerical integration of the shadow degrees of freedom. In this sense, the SWF is not fully explicit, as one cannot write down the result of such an integration. We consider SWF cal-

culations as a class of their own, in between the exact projection methods and the simple and fully explicit wavefunction used here.

Highly effective wavefunctions have been developed over the years for liquid and (nonsymmetric) solid helium. Accurate multi-parameter two- and three- body terms [24–26] result in energies that are nearly exact [26]. However, efficient one-body (lattice) terms that are also exchange-symmetric have not been reported.

The wavefunction that we consider here was proposed specifically for solid ^4He [27]. It has been since then used extensively for importance sampling in projector Monte Carlo methods [28–30]. This wavefunction is a product of the Jastrow term, which accounts for the pair correlations, and a cleverly symmetrized Nosanow-like term. The wavefunction has the the form

$$\psi_{\text{snj}} = \left(\prod_{i < j}^{N_p} f(|\mathbf{r}_i - \mathbf{r}_j|) \right) \left(\prod_k^{N_s} \sum_i^{N_p} g(|\mathbf{r}_i - \mathbf{l}_k|) \right), \quad (1)$$

where N_p is the number of atoms, and N_s is the number of lattice sites, located at \mathbf{l}_k . Position of the i^{th} particle is labeled \mathbf{r}_i . Suitable for our interest in the thermodynamic limit, ψ_{snj} has the translational invariance broken by the lattice site locations \mathbf{l}_k . Notice that the second, product-sum term in Eq. (1), is *not* a permanent, and the computational cost of ψ_{snj} scales only as the square of the number of particles. Pair correlation factors $f(r_{ij})$ can be taken with the pseudopotential either in the McMillan form [31, 32]

$$f(r) = \exp \left[-\frac{1}{2} \left(\frac{b}{r} \right)^5 \right], \quad (2)$$

or in a more involved form with mid-range correlations, as detailed below. Atoms are localized to the lattice sites with factors $g(r)$. We use the Gaussian form

$$g(r) = \exp \left[-\frac{1}{2} \gamma r^2 \right], \quad (3)$$

with parameter γ describing the strength of the site localization.

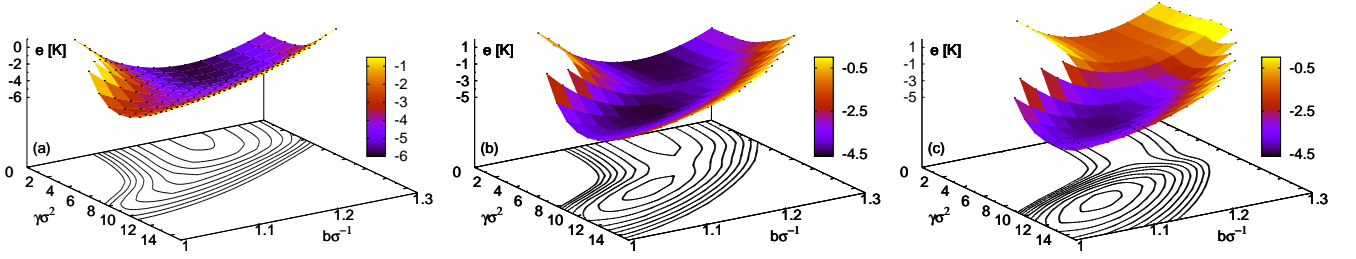


FIG. 1. (Color online) Energy per particle obtained with the two-parameter symmetric wavefunction $\psi_{\text{snj}}^{\{b,\gamma\}}$ given by Eqs. (1-3), as a function of variational parameters b and γ , for three different densities. Parameters are shown in terms of $\sigma = 2.556\text{\AA}$. Simulation used $N = N_s = 900$ particles. (a): density $\rho = 22.2 \text{ nm}^{-3}$ displays a single minimum, at $\gamma = 0$, which corresponds to a liquid phase; (b): intermediate density $\rho = 25.8 \text{ nm}^{-3}$ is in the liquid-solid coexistence region, and has two separate local minima; (c): density $\rho = 29.3 \text{ nm}^{-3}$ displays only one minimum, corresponding to the solid phase. Contours are separated by 0.4 K .

To better understand the structure of ψ_{snj} , we can write the wavefunction in the form

$$\psi_{\text{snj}} = \prod_{i < j}^{N_p} f(r_{ij}) \prod_k^{N_s} S_k, \quad (4)$$

with the site-sums $S_k(\mathbf{r}_1, \dots, \mathbf{r}_{N_p})$ given by

$$S_k = \sum_i^{N_p} g(|\mathbf{r}_i - \mathbf{l}_k|).$$

While each sum S_k depends on the coordinates of all particles, it does not contain interparticle distances. One can view them as a generalized form of one-body correlation factors, in the formal sense that $\nabla_{i \neq j} \cdot \nabla_j S_k = 0$. In this view, Eq. (4) consists of the one- and two-body terms of the general Feenberg form for the trial wavefunction [33, 34]. Equation (4) also emphasizes the flexibility of ψ_{snj} . The number of sites does not need to be equal to the number of particles. One may confine atoms to given regions of the lattice by including these atoms only in some of the sums S_k . Limiting each sum to only one atom recovers the original Nosanow-Jastrow wavefunction [35],

$$\psi_{\text{nj}} = \left(\prod_{i < j}^{N_p} f(|\mathbf{r}_i - \mathbf{r}_j|) \right) \left(\prod_k^{N_s} g(|\mathbf{r}_k - \mathbf{l}_k|) \right), \quad N_s = N_p. \quad (5)$$

The Nosanow-Jastrow wavefunction ψ_{nj} yields good variational energy and has long been used to describe solid ^4He . Unfortunately, ψ_{nj} is not exchange symmetric [36]. The one-body term imposes a heavy penalty for removing an atom away from its “parent” site. A straightforward symmetrization of ψ_{nj} yields poor results [37], or otherwise results in computationally prohibitive wavefunctions.

The lattice structure \mathbf{l}_k , which enters through the site-localization terms $g(\cdot)$, can in principle be seen as a parameter to the wavefunction. In this case one may optimize between different lattice symmetries, or optimize individual site positions. On the other hand, lattice can be seen as an input to the problem. Here we follow the latter path, since we aim to

study the experimentally known zero-temperature solid phase of ^4He . Thus \mathbf{l}_k are located on a geometrically ideal hcp lattice.

We begin with the variational energy optimization of the two-parameter trial wavefunction $\psi_{\text{snj}}^{\{b,\gamma\}}$ given by Eqs. (1–3). The energy is given by

$$E(b, \gamma) = \frac{\langle \psi_{\text{snj}}^{\{b,\gamma\}} | \hat{H} | \psi_{\text{snj}}^{\{b,\gamma\}} \rangle}{\langle \psi_{\text{snj}}^{\{b,\gamma\}} | \psi_{\text{snj}}^{\{b,\gamma\}} \rangle}, \quad (6)$$

with many-body Hamiltonian

$$\hat{H} = -\frac{\hbar^2}{2m_{\text{He4}}} \sum_{i=1}^{N_p} \nabla_i^2 + \sum_{i \neq j} V(r_{ij}),$$

using the HFD–B(HE) pairwise interaction potential proposed by Aziz et al. [38]. The multidimensional integral implied by Eq. (6) was evaluated with a Metropolis Monte Carlo scheme [39, 40]. We performed a direct minimization on a grid of b and γ values, for a range of densities. Three characteristic examples of the energy surface are shown in Fig. 1. At low densities, there is a single minimum with $\gamma = 0$. The wavefunction with $\gamma = 0$ reduces to the translationally invariant Jastrow product and corresponds to a liquid phase. At intermediate densities, an additional local minimum appears at nonzero values of γ , corresponding to a state with broken translational symmetry. This minimum corresponds to a crystalline phase, as was verified from the scaling with N_p of the static structure function. With further increase in density, this second $\gamma \neq 0$ minimum lowers in energy and eventually “overtakes” the liquid $\gamma = 0$ minimum. Thus the solid phase becomes preferred variationally, and the optimized system loses translational symmetry. With the densities increased further still, the liquid minimum disappears. The optimal values of parameters b and γ , shown in Fig. 2 as a function of density, display a clear transition between the solid and liquid states. As our simulated system is finite, the sharpness of this transition is in fact a remarkable occurrence [41–43]. Despite effort, we were not able to detect any smooth rollover between the phases. Technically, the two minima in the energy surface, as shown in Fig. 1 (b), are always distinct. We attribute this

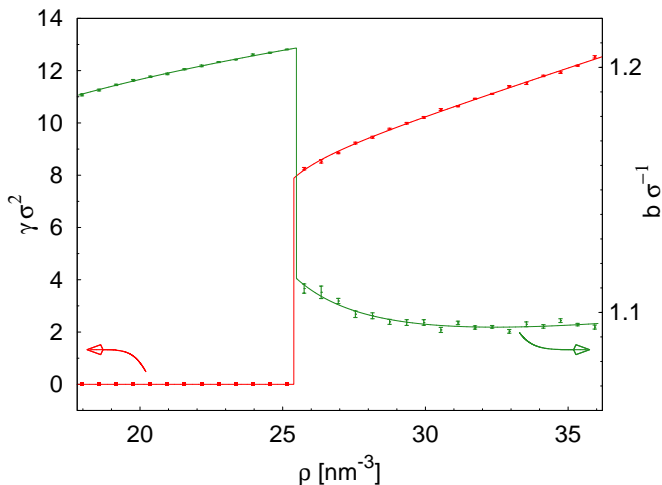


FIG. 2. (Color online) Optimized parameters of the two-parameter symmetric wavefunction given by Eqs. (1–3), as a function of density. Parameters are shown in units of $\sigma = 2.556\text{\AA}$. Left vertical axis corresponds to the value of the site-localization parameter γ , while the right axis shows parameter b .

effect to the fact that the thermodynamic limit is accessible to the finite system through the provided lattice l_k .

Full thermodynamic analysis requires minimization of the Gibbs free energy, which at $T = 0$ equals enthalpy, $G = E + PV$. Enthalpy has to be extracted from the equations of state $E^{\{b,\gamma\}}(\rho)$ computed for each possible set of parameters $\{b, \gamma\}$. The pressure can be computed via

$$P^{\{b,\gamma\}}(\rho) = \rho^2 \frac{\partial E^{\{b,\gamma\}}/N}{\partial \rho}.$$

We solve the above equation for $\rho^{\{b,\gamma\}}(P)$ and find the Gibbs energy for each set of parameters,

$$G^{\{b,\gamma\}}(P) = E + PV = E(\rho^{\{b,\gamma\}}(P)) + PN/\rho^{\{b,\gamma\}}.$$

Next, we minimize $G^{\{b,\gamma\}}(P)$ with respect to variational parameters,

$$G(P) = \min_{\{b,\gamma\}} G^{\{b,\gamma\}}(P).$$

It is possible to show that only the parameters which minimize energy at *some* density will also minimize free energy at any pressure. The parameters which minimize the free energy at a given pressure also provide the density and energy at that pressure. While this method is relatively straightforward, such analysis has not been reported in the past, presumably because of the large underlying computational costs.

We carried out the minimization procedure outlined above for a range of densities. The Gibbs free energy, shown in Fig. 3 as a function of pressure, exhibits a kink characteristic of a first-order phase transition. Corresponding to the weakness of this transition, the kink is subtle yet well-defined. We performed a linear fit to the free energy of the solid phase near the transition, and subtracted this fit from the free energies. The result, which emphasizes the transition, is plotted

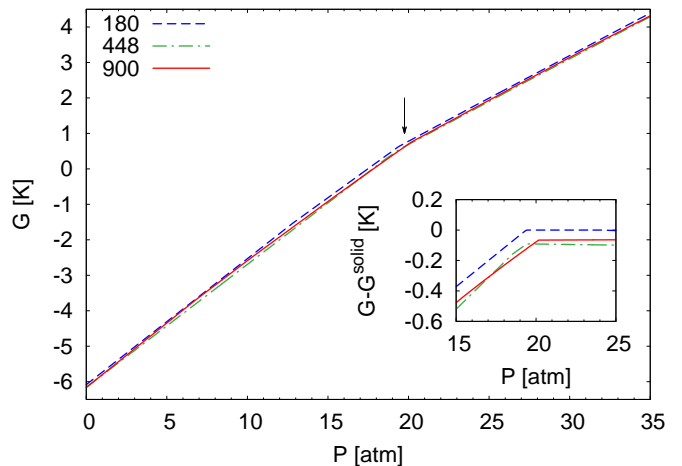


FIG. 3. (Color online) Gibbs free energy, per particle, of the optimized state of the two-parameter symmetric wavefunction given by Eqs. (1–3). Arrow indicates the location of the phase transition. The inset shows the free energies with subtracted linear fit to the solid phase of the 180-particles system.

in the inset to Fig. 3. Somewhat unexpectedly, the transition occurs at a pressure of 20 atm, close to the correct value of 25 atm. This is especially surprising given the simplicity of our two-parameter wavefunction. At the transition pressure, optimized density jumps from the lower density of freezing ρ_f to the higher density of melting ρ_m . At zero temperature, the density discontinuity also provides information about the latent heat ΔE , since $\Delta E = P(1/\rho_f - 1/\rho_m)$. Optimized density $\rho(P)$ is plotted in Fig 4, along with the experimental values [44, 45]. Results are shown for several particle numbers, from $N_p = 180$ to $N_p = 900$. As can be seen, the size effects are moderate and the extrapolated transition pressure for the two-parameter wavefunction is close to 20 atm.

The two-body factors of Eq. (2) account for the short-range behavior of the interaction potential. More accurate two-body factors can be obtained by including mid-range correlations, as in the form proposed in Ref. [46],

$$f(r) = \exp \left[-\frac{1}{2} \left(\frac{b}{r} \right)^5 + \frac{1}{2} s \exp \left(\frac{r - \lambda}{w} \right)^2 \right]. \quad (7)$$

The resulting five-parameter symmetric wavefunction given by Eqs. (1), (3), and (7) was optimized and analyzed as described above. For non-zero optimal γ , the mid-range correlation factor optimizes away, i.e., $s = 0$. That is, the solid phase does not benefit from such correlations. The results for the optimal density at each pressure are shown in Fig. 4. As can be seen, the transition location has improved, and the zero-pressure liquid density has increased, which is closer to the experiment. We also carried the optimization with the two-body factors that included the low-energy phonon contribution along Ref. [47]. Such terms had little influence on the transition location. We conclude that the main source of discrepancy in the pressure of the phase transition stems from

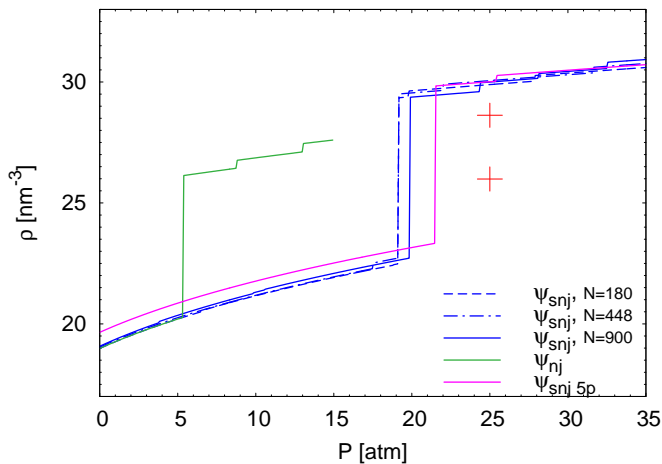


FIG. 4. (Color online) Optimized density as a function of pressure. Blue lines show density for the two-parameter symmetric wavefunction ψ_{snj} for varying number of particles, $N = 180, 448,$ and 900 . The size effects in the transition location are below the statistical error, which is about 1 atm. Purple line shows density for five-parameter symmetric wavefunction with improved pair-correlation factor (7), with transition at 22 bar. Green line shows density for the traditional, non-symmetric Nosanow-Jastrow wavefunction of Eq. (5), with transition at 5 bar. Red cross marks mark experimental melting and freezing densities [44, 45]. The piecewise appearance of data comes from different equations of state $\rho(P)$ selected by the varying pressure-optimized variational parameters; size of the steps is thus indicative of the statistical error.

deficiencies in the two-body factors and the absence of three-body correlation factors in the liquid phase.

The optimization of the thermodynamic potential was also carried out for the two-parameter (unsymmetrized) Nosanow-Jastrow wavefunction ψ_{nj} given by Eqs. (2,3,5). The optimization results are included in Fig.4. Solidification for ψ_{nj} occurs already at 5 bar, a dramatic five-fold departure from the correct location of the transition. In fact, the freezing density ρ_f for ψ_{nj} lies below the correct experimental equilibrium density of helium liquid at vapor pressure. (The equilibrium density is underestimated by all wavefunctions by as much as 15%.) Thus non-symmetric Nosanow-Jastrow wavefunction misses the transition by a wide margin. It should be noted that ψ_{nj} in fact provides lower energies for the solid than the symmetric ψ_{snj} , by up to 1 K. Strict site localization makes ψ_{nj} insensitive to the deficiencies in the two-body factors. The symmetrical ψ_{snj} allows for virtual interstitials and is more sensitive to the form of two-body factor $f(r)$. As the balance between phases amounts to the difference between free energies, to some extent a cancellation occurs, improving the location of the transition for ψ_{snj} .

To summarize, we studied at the variational level the quantum phase transition between superfluid and hcp solid ^4He . The transition properties were determined by optimizing the Gibbs free energy. We used a wavefunction which describes a quantum solid with broken translational symmetry but that is, at the same time, exchange-symmetric. Below the melting

pressure, the optimized wavefunction reduces to a translationally symmetric Jastrow function describing a liquid. Given the simplicity of the wavefunction, it is remarkable that the transition is found at a pressure that is only three to five atm away from the correct experimental value. We attribute the discrepancy to the quality of the pair-correlation terms and the lack of three-body correlations in the liquid phase. These findings strongly support the form given by Eq. (1) as a suitable symmetric wavefunction for describing both a first-order quantum phase transition and a quantum Bose solid.

Authors thank the Barcelona Supercomputing Center (The Spanish National Supercomputing Center – Centro Nacional de Supercomputación) for the provided computational facilities. We acknowledge partial financial support from the DGI (Spain) Grant No. FIS2011-25275 and Generalitat de Catalunya Grant No. 2009SGR-1003. G. E. A. acknowledges support from the Spanish MEC through the Ramon y Cajal fellowship program.

* yaroslav.lutsyshyn@uni-rostock.de;

www.physik.uni-rostock.de/qtmps

† http://bqmc.upc.edu

- [1] E. Kim and M. H. W. Chan, *Nature* **427**, 225 (2004).
- [2] E. Kim and M. H. W. Chan, *Science* **305**, 1941 (2004).
- [3] J. Day and J. Beamish, *Nature* **450**, 853 (2007).
- [4] X. Rojas, A. Haziot, V. Bapst, S. Balibar, and H. J. Maris, *Phys. Rev. Lett.* **105**, 145302 (2010).
- [5] M. H. W. Chan, R. B. Hallock, and L. Reatto, *J. Low Temp. Phys.* **172**, 317 (2013).
- [6] M. Boninsegni, L. Pollet, N. Prokof'ev, and B. Svistunov, *Phys. Rev. Lett.* **109**, 025302 (2012).
- [7] I. Pomeranchuk, *JETP* **20**, 919 (1950).
- [8] R. C. Richardson, *Rev. Mod. Phys.* **69**, 683 (1997).
- [9] B. K. Clark, M. Casula, and D. M. Ceperley, *Phys. Rev. Lett.* **103**, 055701 (2009).
- [10] T. Minoguchi, M. Nava, F. Tramonto, and D. Galli, *J. Low Temp. Phys.* **171**, 259 (2013).
- [11] S. Sachdev, *Quantum Phase Transitions* (Cambridge University Press, 2001).
- [12] P. A. Whitlock, D. M. Ceperley, G. V. Chester, and M. H. Kalos, *Phys. Rev. B* **19**, 5598 (1979).
- [13] M. H. Kalos, M. A. Lee, P. A. Whitlock, and G. V. Chester, *Phys. Rev. B* **24**, 115 (1981).
- [14] L. Vranješ, J. Boronat, J. Casulleras, and C. Cazorla, *Phys. Rev. Lett.* **95**, 145302 (2005).
- [15] A. Sarsa, K. E. Schmidt, and W. R. Magro, *J. Chem. Phys.* **113**, 1366 (2000).
- [16] G. L. Masserini and L. Reatto, *Phys. Rev. B* **35**, 6756 (1987).
- [17] C. Mora and X. Waintal, *Phys. Rev. Lett.* **99**, 030403 (2007).
- [18] S. Vitiello, K. Runge, and M. H. Kalos, *Phys. Rev. Lett.* **60**, 1970 (1988).
- [19] S. Moroni, D. E. Galli, S. Fantoni, and L. Reatto, *Phys. Rev. B* **58**, 909 (1998).
- [20] F. Pederiva, A. Ferrante, S. Fantoni, and L. Reatto, *Phys. Rev. B* **52**, 7564 (1995).
- [21] B. Krishnamachari and G. V. Chester, *Phys. Rev. B* **61**, 9677 (2000).
- [22] T. MacFarland, G. Chester, M. Kalos, L. Reatto, and S. Vitiello,

- Phys. B: Cond. Mat. **194-196**, 525 (1994).
- [23] F. Pederiva, A. Ferrante, S. Fantoni, and L. Reatto, Phys. Rev. Lett. **72**, 2589 (1994).
- [24] V. R. Pandharipande and H. A. Bethe, Phys. Rev. C **7**, 1312 (1973).
- [25] S. A. Vitiello and K. E. Schmidt, Phys. Rev. B **46**, 5442 (1992).
- [26] S. A. Vitiello and K. E. Schmidt, Phys. Rev. B **60**, 12342 (1999).
- [27] C. Cazorla, G. E. Astrakharchik, J. Casulleras, and J. Boronat, New J. Phys. **11**, 013047 (2009).
- [28] C. Cazorla and J. Boronat, Phys. Rev. B **88**, 224501 (2013).
- [29] C. Cazorla, Y. Lutsyshyn, and J. Boronat, Phys. Rev. B **87**, 214522 (2013).
- [30] Y. Lutsyshyn, C. Cazorla, G. E. Astrakharchik, and J. Boronat, Phys. Rev. B **82**, 180506 (2010).
- [31] W. L. McMillan, Phys. Rev. **138**, A442 (1965).
- [32] D. Schiff and L. Verlet, Phys. Rev. **160**, 208 (1967).
- [33] E. Feenberg, Ann. Phys. **84**, 128 (1974).
- [34] C. C. Chang and C. E. Campbell, Phys. Rev. B **15**, 4238 (1977).
- [35] L. H. Nosanow, Phys. Rev. Lett. **13**, 270 (1964).
- [36] One can, in principle, argue that the overlap of any non-symmetrical wavefunction and the true ground state of ${}^4\text{He}$ scales with the number of particles N as $(N!)^{-1}$.
- [37] D. Ceperley, G. V. Chester, and M. H. Kalos, Phys. Rev. B **17**, 1070 (1978).
- [38] R. A. Aziz, F. R. W. McCourt, and C. C. K. Wong, Mol. Phys. **61**, 1487 (1987).
- [39] Y. Lutsyshyn, (2013), arXiv:1312.1282.
- [40] We employed a CUDA parallelization for graphical processing unit as described in Ref. [39], and used a cluster of Nvidia GPU to carry out the integrals of Eq. (6) to a sufficiently high accuracy. All calculations were carried out to at least 10 mK error in energy per particle.
- [41] M. Campostrini, J. Nespolo, A. Pelissetto, and E. Vicari, Phys. Rev. Lett. **113**, 070402 (2014).
- [42] M. Mueller, W. Janke, and D. A. Johnston, Phys. Rev. Lett. **112**, 200601 (2014).
- [43] G.-D. Lin, C. Monroe, and L.-M. Duan, Phys. Rev. Lett. **106**, 230402 (2011).
- [44] R. D. B. Ouboter and C. N. Yang, Physica **144**, 127 (1987).
- [45] D. O. Edwards and R. C. Pandorf, Phys. Rev. **140**, A816 (1965).
- [46] L. Reatto, Nucl. Phys. A **328**, 253 (1979).
- [47] W. P. Francis, G. V. Chester, and L. Reatto, Phys. Rev. A **1**, 86 (1970).